

Temperature Dependence of Electrical Resistivity in Carbon Nanofiber/Unsaturated Polyester Nanocomposites

Toshiaki Natsuki^{1*}, Qing-Qing Ni¹ and Shi-Hong Wu²

¹ Dept. of Functional Machinery and Mechanics,
Shinshu University,
3-15-1 Tokida, Ueda 386-8567, Japan

² Maruzen Electric co., Ltd.
2-16 higasiarioka, Itami 664-0845, Japan

* *Corresponding author*

Abstract

This paper described the temperature dependence of electrical resistivity for carbon nanofiber (CNF)/unsaturated polyester resin (UPR) nanocomposites prepared by a solvent evaporation method. It was found that the CNF/UPR nanocomposites had quite low electrical percolation threshold due to CNFs having a large aspect ratio and being well dispersed into the UPR matrix. A Sharp decrease in the electrical resistivity was observed at about 1 wt% CNF content. The influence of CNF content on the electrical resistivity was investigated as a function of temperature in detail. The nanocomposites showed a positive temperature coefficient (PTC) effect for the resistivity, and had a strong temperature dependence near the percolation threshold. When the number of thermal cycles was increased, the electrical resistivity decreased and had a weak temperature dependence, especially in the case of melting temperature. Moreover, the size influences of CNFs on the electrical properties of nanocomposites were analyzed and discussed.

Key words: Carbon nanotubes, Electrical properties, Nanocomposites

INTRODUCTION

Carbon nanotubes (CNTs) have attracted great interest in the development of applications due to their exceptional mechanical, electrical and thermal properties [1-4]. There are many ways to produce carbon nanotubes and nanofibers (CNFs), such as arc-discharge, laser vaporization, chemical vapor deposition (CVD), etc. The most promising mass production-wise method is the CVD that uses metal catalytic particles, and is known as catalytic CVD (CCVD). This process allows control over a wide of tube diameters, layer numbers, and tube lengths. The vapor grown carbon fibers (VGCFs) by the CCVD method are characterized as with highly preferred orientation of their graphitic basal plane parallel to the fiber axis and with annular ring texture in the cross section [5].

Carbon nanotubes are considered to be an ideal filler material for nanocomposites. Some carbon nanotube composites are already applied for sporting goods, and available on the market. Recently, there is considerable interest in studying the electrical behavior of nanocomposites containing CNFs since they could dramatically improve the electrical conductivity of polymers by just adding a little CNFs. Many studies on the electrical properties of polymer matrix composites filled with carbon fibers or CNFs have been reported [6-9]. The carbon-filled conductive polymers could be widely used for static dissipative, semiconductive, electromagnetic interference (EMI) and radio frequency interference (RFI) shielding applications [8, 9]. In a changing temperature environment, the conductive stabilization for composites is quite important for their actual applications. Hou et. al. [10] have studied the performance stabilization of conductive polymer composites filled with carbon black (CB). They obtained that the *in situ* grafting of acrylic acid at the filler/matrix interaction could effectively improve the short-term performance stability of the composites. Another important property of the electrically conductive composites was a positive temperature coefficient (PTC) effect, which meant the electrical resistivity of the composites increases during the heating process. PTC materials have widespread applications, including sensors, self-regulating heaters and switching materials. The PTC mechanism was due to the difference in the coefficients of thermal expansion between the fillers and the matrix. The thin gaps between the adjacent conductive fillers, or the breakdowns of percolation networks increased with an increase in Joule heating or environment temperature in the case of the difference in thermal expansion. An expansion of the polymer matrix during heating increased the width of the gaps, and thus hindered the process of the electron tunneling [11]. Hindermann-Bischoff et. al. [12] have reported that the electrical resistivity of CB filled high density polyethylene increased significantly when the composites were heated to the melting temperature of the matrix. A sufficient amount of CB particles were required to ensure that the gaps between CB particles or their aggregates were small enough to allow electron tunneling. Zhang et. al [11] have studied the temperature

dependence of the electrical resistivity for the carbon black(CB)/ultra-high molecular weight polyethylene (UHMWPE) composites. They reported that the degree of the intermixing between CB and UHMWPE particles plays an important role in determining the electrical properties of the composites. The temperature dependence of the electrical resistivity has been widely studied for CB filled various types of polymer [11, 12]. However, there were few reports on the mechanism of PTC effects in nanocomposites, especially on the nanocomposites filled with VGCF. The electrical conductivity of polymer/multi-walled carbon nanotube (MWCNTs) composites has recently been studied [13, 14]. Lisunova et. al [13] obtained the ultralow electrical percolation threshold in ultrahigh molecular weight polyethylene/MWCNTs composites. The PTC effect was observed in the region of temperatures higher than melting point. Compared with CB, the PTC intensity and repeatability of nanocomposites were dramatically improved by the addition of a small amount of MWNTs [14].

The purpose of this paper is to examine the effect of CNF size on the electrical properties in the nanocomposites. Two types of CNFs used in this work were VGCF and vapor grown carbon nanofibers (VGNF) produced by the CCVD method. The nanocomposites were prepared by a solution evaporation method. Moreover, the temperature dependence of the electrical properties for the nanocomposites was investigated as a function of filler contents so as to understand the percolation behavior, the temperature-resistivity and current-voltage characteristics.

EXPERIMENTAL PROCEDURE

Materials

Two types of CNFs used as conductive fillers were VGCFs and VGNFs produced by Showa Denko Co., Ltd. Japan. The VGCFs were analyzed by scanning electron microscopy (SEM), and their average diameter was about 150 nm and the length was 10-20 μm . The VGNFs were about 80 nm in diameter and less than 20 μm in length. The resin used as matrix was unsaturated polyester resin (UPR), and the hardening agent was PERMEK, produced by NOF Co., Ltd. Japan. The properties of CNFs and UPR were listed in Table 1.

Preparation of Nanocomposite Sheets

The nanocomposite sheets were fabricated using a solvent evaporation method. According to the weight content, a fixed quantity of CNFs was well dispersed in aqueous ethanol by an ultrasonic stirring. Then, the unsaturated polyester resin was poured into the CNFs-erhanol solution and stirred well with a glass rod. Moreover, the filled CNF mixture was ultrasonicated at room temperature for 3 hours. In order to evaporate the ethanol, the mixtures were placed in a muffle furnace at 80 $^{\circ}\text{C}$ for 4 hours. Subsequently, the hardening agent was blended into the mixtures at room temperature.

Finally, a sheet with 1 mm thickness was modeled and cured at room temperature for 24 hours, immediately followed by 100 °C for 1 hour.

Electrical Resistivity Measurements

In our experiment, the volume resistivity of the CNF/UPR nanocomposites was measured using the two-terminal method. The rectangular bar specimens 30×5×1 mm³ were cut from the nanocomposite sheet. Silver paste was coated on the surfaces of the specimens in order to ensure good electrical contacts between the materials surface and the copper electrodes. Five samples at each concentration were measured for the temperature dependence of the electrical resistivity, using a digital multimeter VOA7510 (IWATSU Co., Ltd. Japan). In the case of the dynamic conductivity measurements of temperature changes, the specimens attached to the copper electrodes were placed in an oven, controlling the temperature changes from room temperature to 190 °C by computer program. The temperature dependence of the electrical resistivity was measured at a heating rate of 2 °C/min. A direct current (DC) voltage source was used to measure the time dependence of the electrical resistivity. Figure 1 illustrates the measurement system for the temperature dependent of the electrical resistivity. The current-voltage characteristics were carried out under continuous direct current voltage power changed from 5 to 100 V.

Morphology Observation

Morphology of the brittle fractured surfaces was observed using a Hitachi S-510 scanning electron microscopy (SEM). The samples were sputtered with gold-palladium prior to observation.

RESULTS AND DISCUSSION

Morphology of Nanocomposites

Figure 2 shows SEM photomicrographs of fracture surfaces of unsaturated polyester resin filled with 4 wt% contents of VGCFs (a) and VGNFs (b), respectively. The darker regions correspond to the unsaturated polyester resin and the brighter regions to the carbon nanofibers. The SEM micrographs show that both VGCFs and VGNFs are randomly oriented and dispersed uniformly within the polymer matrix. In addition, the CNFs are observed to form interconnecting structures. The micrograph observation can show that the CNF/UPR nanocomposites have low percolation threshold with CNF content less than 4 wt%.

Electrical Resistivity

Figure 3 shows the effect of CNF contents on volume resistivity at room temperatures. It can be seen that the volume resistivity of both VGCF/UPR and

VGNF/UPR nanocomposites exhibits a percolation behavior because larger decreases in the resistances are observed. To determine the concentration threshold, a power relation $(\rho - \rho_c)^{-t}$ is used, where ρ is the mass fraction and ρ_c is the critical fraction corresponding to the percolation threshold, and t is the critical exponent. In the case of VGNF/UPR nanocomposites, the percolation threshold occurs at about 2.0 wt%. The percolation threshold of VGCF/UPR nanocomposites exhibits a slightly lower than that of VGNF/UPR nanocomposites. This characteristic can be attributed to the aggregation of VGNFs. The entanglements and the van der Waals interactions between the nanofibers result in VGNF aggregates and formation of large clusters. Thus, the VGNFs are more difficult to be dispersed uniformly compared with the VGCFs because the VGNFs have smaller diameter and larger aspect ratio than VGCFs have. Electron tunneling between conductive fillers could be another reason why CNF composites have lower percolation threshold and high electrical conductivity [15, 16]. The conducting pathways in nanocomposites filled with CNFs are not only physical contacts between themselves, but also connections between the CNFs with very small intervals across which electrons can tunnels. The same behavior of the voltage-current characteristics between VGCF and VGNF needs to be investigated further.

Voltage-Current Characteristics

The voltage-current characteristics were measured at room temperature for the CNF/UPR nanocomposites with different contents of CNFs. Figure 4(a) and (b) show the voltage-current characteristics of the nanocomposites with 2~5 wt% content of VGCF and VGNF, respectively. The voltage-current characteristics for the nanocomposites with 2~3 wt% are found to be linear relations that obey Ohm's law. In the case of the nanocomposites with 4~5 wt% CNFs, however, the voltage-current relationships become slightly nonlinear with increasing voltage. This is because the nanocomposites filled with high CNF contents easy to generate large joule heat when the electric field increase, leading to a decrease in the conductivity. The conductivity mechanism of CNF composites with 4~5 wt% content is mainly ohmic conductivity due to the direct contacts between CNFs. This can be observed from the SEM microphotographs shown in Fig.2.

Temperature Dependence of the Electrical Resistivity

Figure 5 shows the temperature dependence of CNF composites on the electrical resistivity as a function of CNF contents. It is seen that the resistances are dependent on the CNF contents. The temperature dependence of the electrical conductivity exhibits PTC effects, but not quite stronger. The main reason of the PTC effects was supposed to be a separation of interfiber contacts [17].

The temperature dependence of the electrical conductivity maybe explained by a general theory of the thermal fluctuations. The conductivity of the junction is given by [18]

$$\rho = \rho_0 \exp[-T_1 / (T + T_0)] \quad (1)$$

where the constants ρ_0 , T_1 and T_0 depend essentially on the characteristics of the tunnel junctions, which are supposed to be functions of various parameters such as filling factor, filler size and shape, sample processing [19].

Based on the conductive mechanism [15, 19], the electrical conduction in CNF/UPR nanocomposites is mainly composed of two parts: one is Ohmic resistance of CNFs owing to direct contacts between fibers, and another is tunneling resistance determined by the width of the insulating resin layer around CNFs. Volumetric expansion due to heat increases gape width between contiguous CNFs and reduces the number of conductive pathways, resulting an increase in the volume resistance. Therefore, the PTC effects take place mainly owing to electron tunneling between isolated conductive fillers. In this work, the negative temperature coefficient (NTC) effects were not observed. This is because the NTC effects can be restricted by chemical crosslinking, which increases the viscosity of the matrix and produces a gel like network, consequently resulting in the stabilization of filler dispersion in polymer matrix [20].

In order to examine how sensitive and what extent the resistance response will be after being stimulated by the temperature change, the relative resistivity (ρ_r) can be used to characterize the intensity of the PTC effect:

$$\rho_r = \log(\rho_{180^\circ} / \rho_{25^\circ}) \quad (2)$$

where ρ_{180° and ρ_{25° are the resistances of the composites at 180°C and 25°C, respectively. Figure 6 shows the influence of CNF contents on the relative resistivity. A larger PTC effect is observed for the nanocomposites with a lower VGCF content. In this case, the electrical conductivity is regarded to be partially caused by the electron tunneling through gap separations between VGCFs, resulting in the larger PTC effect. In the case of a larger VGCF content, however, the conductive pathways between VGCFs are hardly to be broken up. Therefore, the PTC effect of nanocomposites with a high content is weaker than that of nanocomposites with a low content. Note that the intensity of the PTC effect of VGNF/UPR nanocomposites is weaker than that of VGCF/UPR nanocomposites, especially in the case of about 2 wt% CNFs near the percolation threshold. The result may be explained by temperature stabilization. The VGNFs have higher surface-to-volume ratio compared to the VGCFs due to their small size. This shows that the interface strengths of VGNFs are larger than those of the

VGCFs, leading to the temperature stabilization of filler dispersions in the polymer matrix.

Influence of Heat Cycle

In order to examine the reproducibility of the electrical conductivity and the PTC, the resistivity measurement was carried out by several heating/cooling cycles. Figure 7 (a) and (b) show the temperature dependence of the volume resistivity during the repeated heating/cooling cycles for the nanocomposites with VGCFs and VGNFs, respectively. The PTC effects of the nanocomposites are influenced by the heating/cooling cycles. Especially, the temperature response of the resistivity decreases largely after the first heating/cooling cycle, and becomes insensitive to the cycle numbers with an increase in the heating/cooling cycle. The different PTC effects caused by the cycle times are due to the further intermixing of CNFs at higher temperature. The CNFs in the polymer matrix are easy to agglomerate by Van der Waals force and Brownian motion at high temperature beyond the glass transition or the melting temperature, and finally form interfiber networks. The effects of the thermal cycle numbers on the volume resistivity of CNF/UPR nanocomposites are shown in Fig.8. It can be seen that the PTC effects of the VGNF/UPR nanocomposites have higher stability than those of the VGCF/UPR nanocomposites.

Characteristic of the Electrical Resistivity versus Annealing Time

The time dependence of the electrical resistivity annealed at 190 °C for VGCF/UPR and VGNF/UPR nanocomposites with 3 wt% content is shown in Fig.9. It is observed that initial resistivities of the nanocomposites increase drastically with annealing time. After the resistances reach a maximum, the resistivities were decreased by 30% with further increase in annealing time. This can be explained by the thermal expansion of matrix and the relaxation of polymer chains. The gap width around conductive nanofibers increases since the polymer matrix expands when heated to 190 °C, resulting in an increased resistivity of the VGNF/UPR nanocomposites. When the thermal expansion becomes more stability with increasing time, the CNFs in the polymer matrix form a conductive network due to Brownian motion at melting temperature. The volume resistivity of the nanocomposites decrease, therefore, leading to the stabilized resistance values.

CONCLUSIONS

In this work, we fabricated the CNF/UPR nanocomposites by a solution evaporation method, and their PTC effects were investigated. The electrical characteristics of the nanocomposites are summarized as follows:

The temperature dependences of both VGCF/UPR and VGNF/UPR nanocomposites

on CNF contents have very low electrical percolation thresholds because the CNFs have large aspect ratios and electron tunnelings.

The gap width between contiguous CNFs becomes enlarged since the thermal expansion of the UPR matrix is much larger than that of the CNFs. Therefore, the nanocomposites have a positive temperature coefficient effect, but not show a negative temperature coefficient effect. The larger PTC effects are observed for the nanocomposites with a low VGCF content, near the percolation threshold.

The PTC effects of the nanocomposites decrease with increasing number of the heating/cooling cycles because of the thermal stabilization of CNFs within a polymer matrix. The electrical resistivity increases drastically to reach maximum with annealing time, and then decreases slowly.

ACKNOWLEDGMENT

This work was supported by Grant-in-Aid for Global COE Program by the Ministry of Education, Culture, Sports, Science, and Technology.

REFERENCES

- [1] M.M.J Treacy, T.W. Ebbesen and J.M., Gibson, *Nature* **381**, 678 (1996).
- [2] E.W. Wong, P.E. Sheehan and C.M. Liebe, *Science* **277**, 1971 (1997).
- [3] L. Vaccarini, C. Goze, L. Henrard, E. Hernandez, P. Bernier and A. Rubio, *Carbon* **38**, 1681 (2000).
- [4] E.T. Thostenson, Z. Ren and T.W. Chou, *Comp. Sci. Tech.* **61**, 1899 (2001).
- [5] Y. Bin, M. Mine, A. Koganemaru, X. W. Jiang and M. Matsuo, *Polymer* **47**, 1308 (2006).
- [6] T. Natsuki, M. Endo and T. Takahashi, *Physica A* **352**, 498 (2005).
- [7] J.N. Coleman, J. Fraysse, P. Fournet, M. Cadek, A. Drury, S. Hutzler, S. Roth and W.J. Blau, *J. Appl. Phys.* **92**, 4024 (2002).
- [8] C.C. Ma, Y.L. Huang, H.C. Kuan and Y.S. Chiu, *J. Polym. Sci. Part B: Polym. Phys.* **43**, 345 (2005).
- [9] N.B. Janda, J.M. Keith, J.A. King, W.F. Perger and T.J. Oxby, *J. Appl. Polym. Sci.* **96**, 62 (2005).
- [10] Y.H. Hou, M.Q. Zhang and M.Zh. Rong, *J. Appl. Polym. Sci.* **89** 2438 (2003).
- [11] C. Zhang, C.A. Ma, P. Wang and M. Sumita, *Carbon* **43**, 2544 (2005).
- [12] M. Hindermann-Bischoff, and F. Ehrburger-Dolle, *Carbon* **39**, 375 (2001).
- [13] M.O.Lisunova, Ye.P. Mamunya, N.I. Lebovka, A.V. Melezhyk, *Europ. Polym. J.* **43** 949 (2007).
- [14] J.-H. Lee, S. K. Kim and N. H. Kim, *Scrip. Mater.* **55** 1119 (2006).
- [15] D. Toker, D. Azulay, N. Shimoni, I. Balberg and O. Millo, *Phys. Rev. B* **68**, 041403 (2003).
- [16] P. Sheng, E.K. Sichel and J. I. Gittleman. *Phys. Rev. Lett.* **40**, 1197 (1978).
- [17] Y. Chekanov, R. Ohnogi, S. Asai and M. Sumita, *J. Mater. Sci.* **34**, 5589 (1999).
- [18] P. Sheng, E.K. Sichel and J.I. Gittleman, *Phys. Rev. Lett.* **40**, 1197 (1978).
- [19] P. Sheng, *Phys. Rev. B* **21**, 2180 (1980).
- [20] W. Di, G. Zhang, J. Xu, Y. Peng, X. Wang and Z. Xie, *J. Polym. Sci. Part B: Polym. Phys.* **41**, 3094 (2003).

Figure captions

Figure 1 Illustration of the conductivity measurement for dynamic electrical resistivity.

Figure 2 SEM micrographs of fracture surfaces for nanocomposites with CNF contents:
(a) 4wt% VGCF; (b) 4wt% VGNF.

Figure 3 Changes in the electrical resistivity vs. weight content for VGCF/UPR and VGNF/UPR nanocomposites.

Figure 4 Voltage-current characteristics in CNF nanocomposites: (a) VGCF/UPR; (b) VGNF/UPR.

Figure 5 Logarithm of volume resistivity versus temperature for CNF nanocomposites:
(a) VGCF/UPR; (b) VGNF/UPR.

Figure 6 Influences of CNF contents on the relative resistivity in CNF/UPR nanocomposites.

Figure 7 Effects of the thermal cycles on the temperature dependence of the volume resistivity in CNF composites with 3 wt% content: (a) VGCF/UPR; (b) VGNF/UPR.

Figure 8 Variation of the volume resistivity with the number of thermal cycles in CNF/UPR nanocomposites with 3 wt% content.

Figure 9 Time dependence of the volume resistivity for CNF/UPR nanocomposites at the ambient temperature 190 °C.

Table 1 Material properties of carbon nanofibers and unsaturated polyester resin

Figure 1.(T. Natsuki)

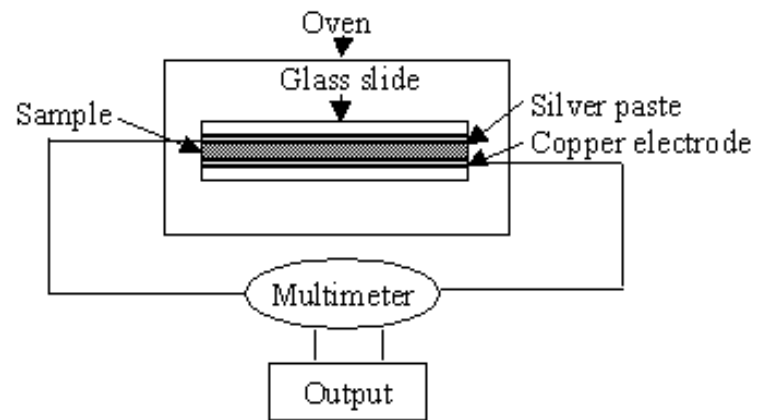


Figure 2. (T. Natsuki)

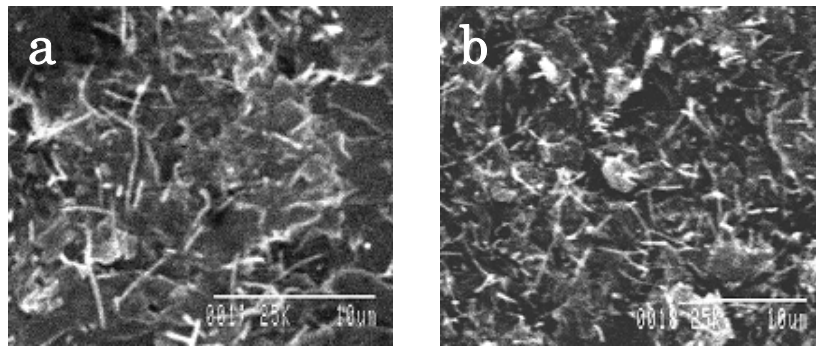


Figure 3. (T. Natsuki)

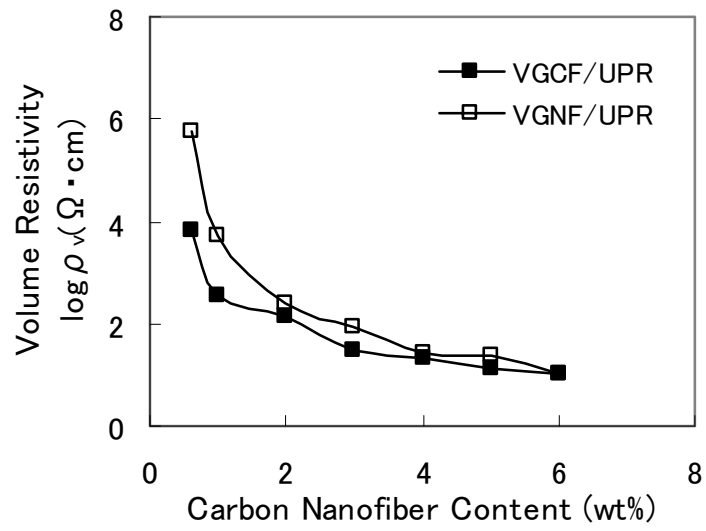


Figure 4 (T. Natsuki)

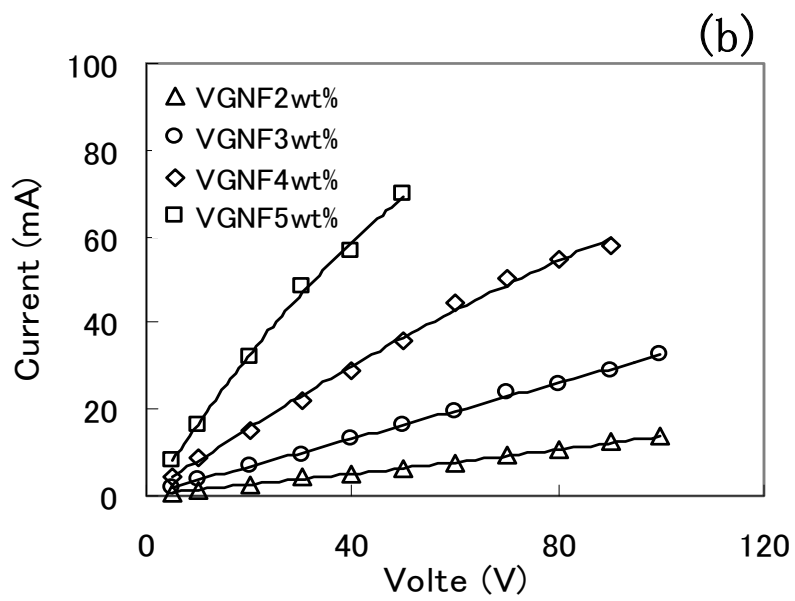
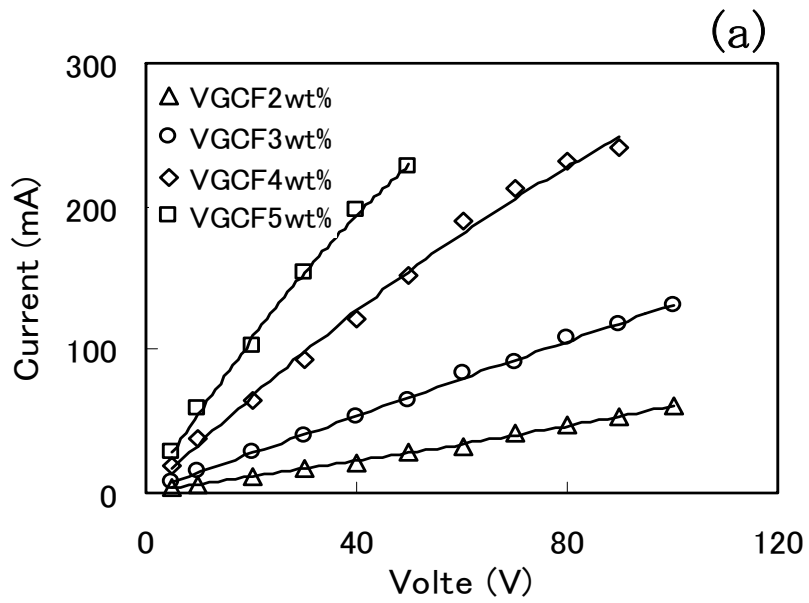


Figure 5 (T. Natsuki)

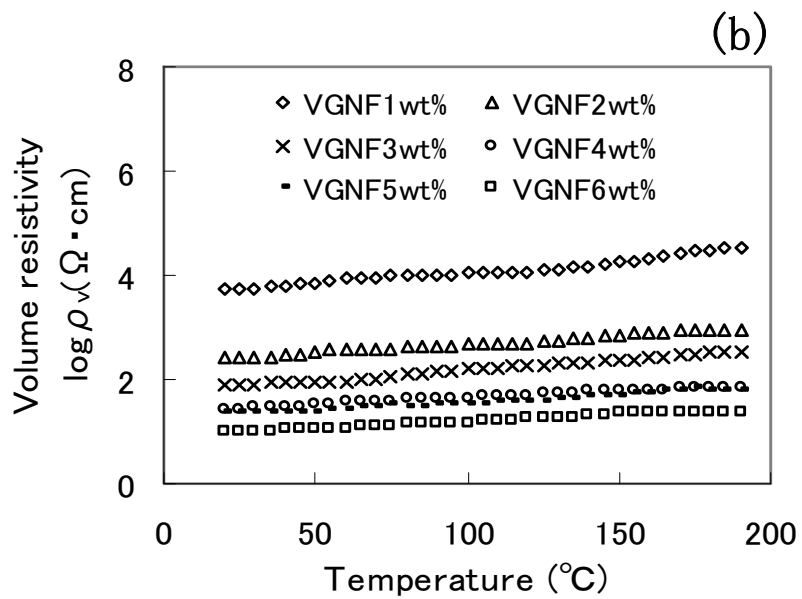
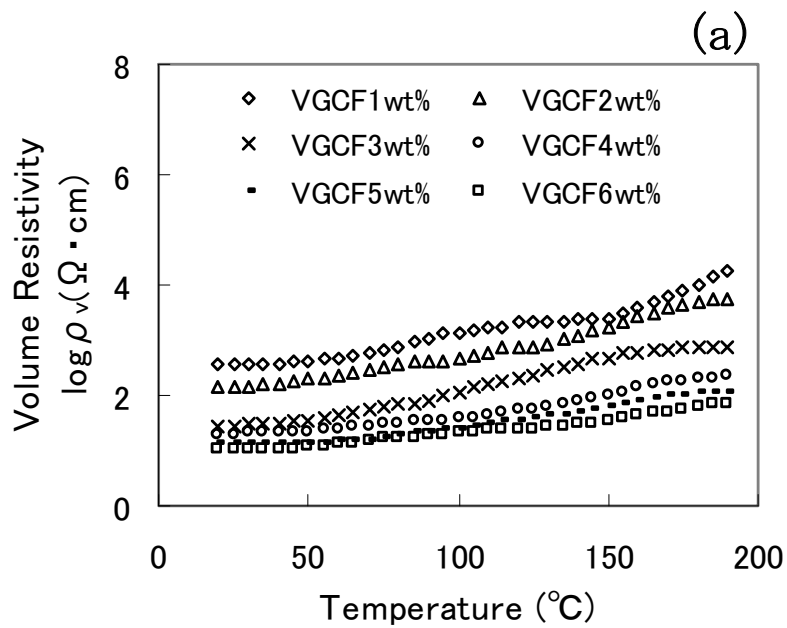


Figure 6 (T. Natsuki)

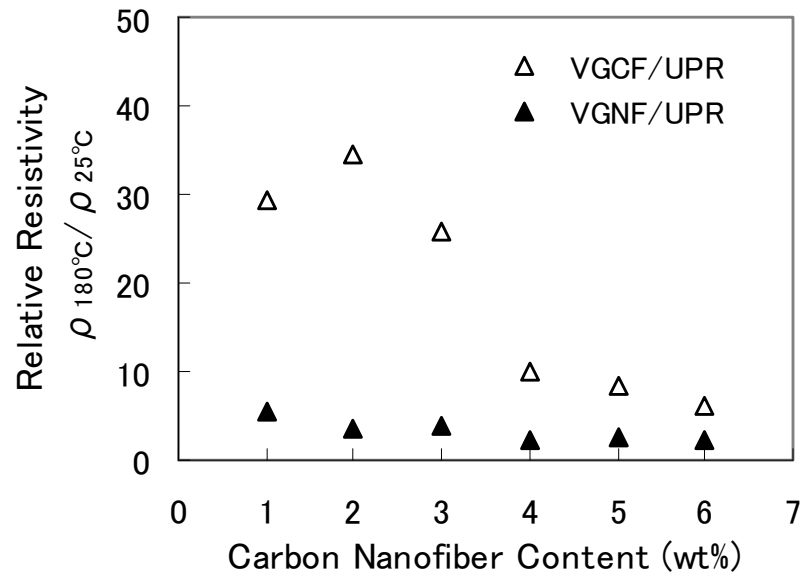


Figure 7 (T. Natsuki)

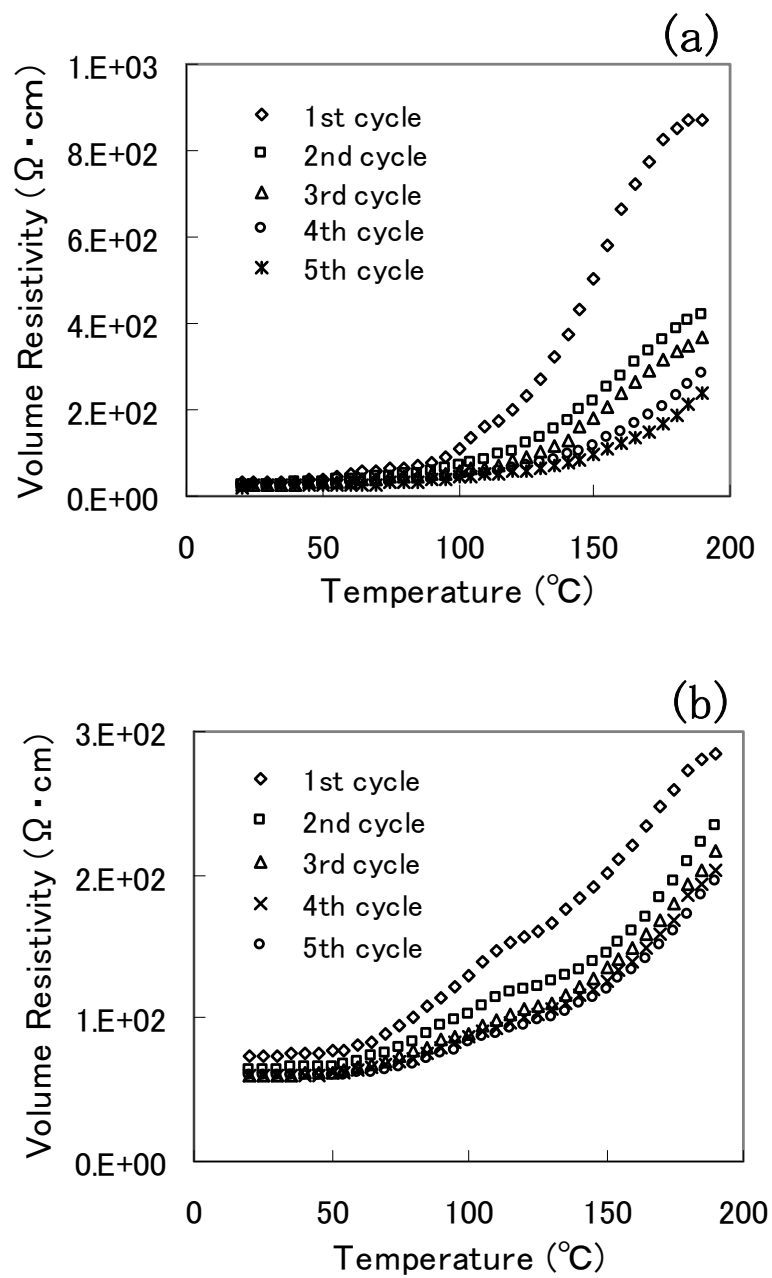


Figure 8 (T. Natsuki)

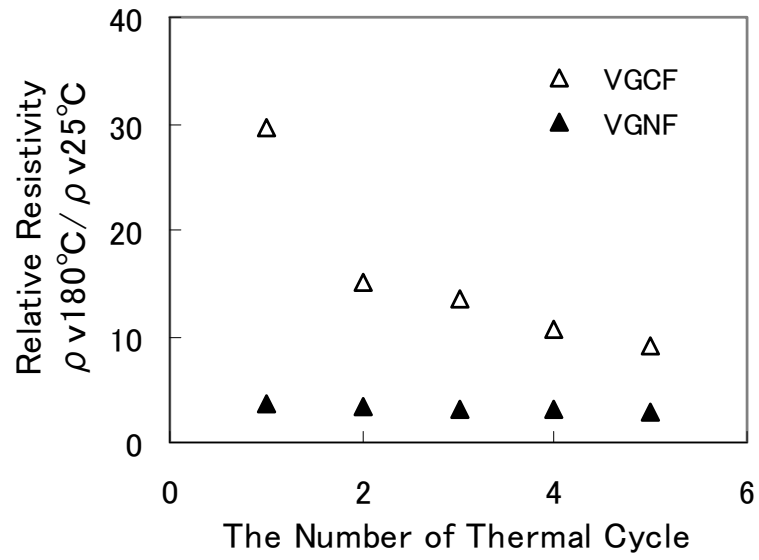


Figure 9 (T. Natsuki)

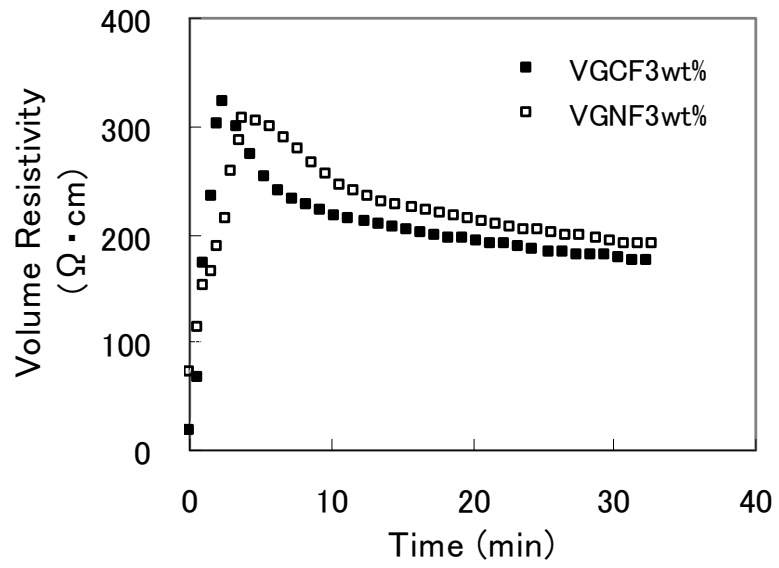


Table 1 (T. Natsuki)

Properties	CNF	UPR
	VGCF/VGNF	
Density (g/cm ³)	2.0 / 2.0	1.0
Diameter (nm)	150 / 80	–
Length (mm)	20 / <20	–
Coefficient of thermal expansion (1/° C)	4×10 ⁻⁶	5×10 ⁻⁵